⑫ LEVEL Ⅱ

TECHNICAL REPORT H-78-22

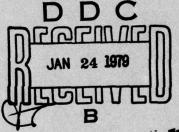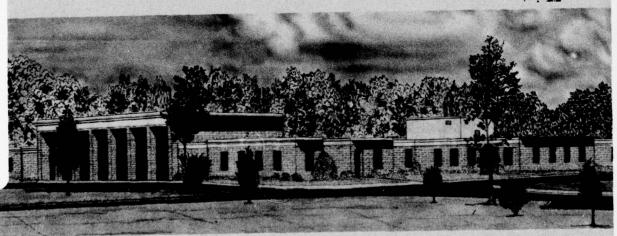# NUMERICAL SIMULATION OF THE COOS BAY-SOUTH SLOUGH COMPLEX

by

H. Lee Butler

Hydraulics Laboratory
U. S. Army Engineer Waterways Experiment Station
P. O. Box 631, Vicksburg, Miss. 39180

December 1978
Final Report

Approved For Public Release; Distribution Unlimited

Prepared for U. S. Army Engineer District, Portland
Portland, Oregon 97208

SECURITY CLASSIFICATION OF THIS PAGE (When Data Entered)

REPORT DOCUMENTATION PAGE		READ INSTRUCTIONS BEFORE COMPLETING FORM
1. REPORT NUMBER Technical Report H-78-22	2. GOVT ACCESSION NO.	3. RECIPIENT'S CATALOG NUMBER
4. TITLE (and Subtitle) NUMERICAL SIMULATION OF THE COOS BAY-SOUTH SLOUGH COMPLEX		5. TYPE OF REPORT & PERIOD COVERED Final report
		6. PERFORMING ORG. REPORT NUMBER
7. AUTHOR(s) H. Lee Butler		8. CONTRACT OR GRANT NUMBER(s)
9. PERFORMING ORGANIZATION NAME AND ADDRESS U. S. Army Engineer Waterways Experiment Station Hydraulics Laboratory P. O. Box 631, Vicksburg, MS 39180		10. PROGRAM ELEMENT, PROJECT, TASK AREA & WORK UNIT NUMBERS
11. CONTROLLING OFFICE NAME AND ADDRESS U. S. Army Engineer District, Portland P. O. Box 2946 Portland, OR 97208		12. REPORT DATE December 1978
		13. NUMBER OF PAGES 123
14. MONITORING AGENCY NAME & ADDRESS(if different from Controlling Office)		15. SECURITY CLASS. (of this report) Unclassified
		15a. DECLASSIFICATION/DOWNGRADING SCHEDULE

16. DISTRIBUTION STATEMENT (of this Report)

Approved for public release; distribution unlimited.

128 p.

17. DISTRIBUTION STATEMENT (of the abstract entered in Block 20, if different from Report)

WES-TR-H-78-22

18. SUPPLEMENTARY NOTES

19. KEY WORDS (Continue on reverse side if necessary and identify by block number)

Coos Bay	Navigation channels
Estuaries	Numerical simulation
Hydrodynamics	South Slough, Ore.
Inlets (Waterways)	Tidal inlets
Mathematical models	Tidal models

20. ABSTRACT (Continue on reverse side if necessary and identify by block number)

Coos Bay Inlet, located on the south central coast of Oregon, provides tidal flow to two estuary systems: Coos River to the north and South Slough to the south. The upper reaches of South Slough constitute a National Marine Sanctuary, administered by the National Oceanographic and Atmospheric Administration. Charleston Harbor is located at the entrance into South Slough and is affected by continual shoaling problems within the harbor entrance channel.

(Continued)

DD FORM 1473 EDITION OF 1 NOV 65 IS OBSOLETE   Unclassified

79 01 22 088

038 100

20. ABSTRACT (Continued)

A two-dimensional numerical tidal model (WIFM) was used to investigate the tidal hydrodynamics of the inlet complex. Due to the nature of the complex geometry of the Coos Bay area, it was necessary to develop a capability of computing the tidal regime on a variable grid system. The primary objective of this study was to apply WIFM to the Coos Bay-South Slough complex to predict quantitatively the hydrodynamics (exclusive of sediment transport and wave action) of the tidal flow in the system and hence draw a comparison between existing conditions and alternate improvement plan conditions. In general, the improvement plans provide for:

    a. Construction of specified navigation channels.

    b. Alternate breakwater extensions west of the entrance channel.

    c. Alternate detached groins east of the entrance channel.

Five alternate plans (plan 1 and plans A-D) were tested, and the results show that the introduction of any of the improvement plans as proposed would not produce any detrimental impact to tidal circulation in South Slough. The greatest effect on the hydrodynamics of the total system would occur with the installation of plan 1. Results for plans A-D indicate that the combination of a Charleston breakwater extension and one or more groins on the east side of Charleston Channel would best meet the District's needs in that they permit more control over the alignment of the Charleston Channel. Time histories of tide elevations and velocities are presented for selected stations throughout the Coos Bay-South Slough complex. Sample circulation patterns for four instances in the tidal cycle are presented for the verification conditions and for each plan. Total discharge through several key ranges in the system is graphed as a function of time. A wave refraction analysis, using a linear wave refraction model, was performed to determine wave energy levels penetrating the entrance to Coos Bay Inlet. Results are tabulated for six initial deepwater directions and six periods. An attempt was made to compute wave orthogonals extending into Coos Bay Inlet. Only those shallow-water waves whose azimuth is aligned with the entrance channel would propagate within the inlet system. Results obtained by the linear wave refraction code are very limited for sites such as Coos Bay due to the complex channel formation extending outward from the inlet jetties and shoal areas adjacent to the main channel as it progresses eastward toward Barview.

PREFACE

The model investigation described herein was authorized by the U. S. Army Engineer District, Portland, and conducted at the U. S. Army Engineer Waterways Experiment Station (WES) in the Wave Dynamics Division (WDD), Hydraulics Laboratory, under the direction of Mr. H. B. Simmons, Chief of the Hydraulics Laboratory, and Dr. R. W. Whalin, Chief of the Wave Dynamics Division.

The investigation was performed and this report prepared by Mr. H. Lee Butler, WDD. Mr. George Fisackerly, Estuaries Division, supervised the field survey. The numerical computations associated with this work were performed on a Control Data Cyber 176 located at the Air Force Weapons Laboratory (AFWL), Kirtland Air Force Base, New Mexico.

Commander and Director of WES during the course of the investigation and the preparation and publication of this report was COL John L. Cannon. Technical Director was Mr. Fred R. Brown.

CONTENTS

CONVERSION FACTORS, U. S. CUSTOMARY TO METRIC (SI) UNITS OF MEASUREMENT

U. S. customary units of measurement used in this report can be converted to metric (SI) units as follows:

Multiply	By	To Obtain
feet	0.3048	metres
feet per second	0.3048	metres per second
square miles (U. S. statute)	2.589988	square kilometres
square feet per second	0.09290304	square metres per second
feet per second per second	0.3048	metres per second per second

Figure 1. Location of Coos Bay Inlet in southwest Oregon

NUMERICAL SIMULATION OF THE COOS BAY-SOUTH SLOUGH COMPLEX

PART I: INTRODUCTION

Background

1. This study, funded by the U. S. Army Engineer District, Portland, Engineering Division (NPPEN), was initiated for the purpose of investigating the effect of several alternative training dikes and/or breakwaters on tidal circulation in the Coos Bay-South Slough area. Coos Bay Inlet is a natural inlet located on the south central coast of Oregon (Figure 1). The inlet traffics heavy shipping up the Coos Bay River to North Bend and small craft (commercial fishing and pleasure craft) to Charleston Harbor just south of the inlet entrance. Depths in the entrance channel and the Coos River ranges reach 60 ft* NGVD (National Geodetic Vertical Datum). This reference to depth means 60 ft below the plane of NGVD where NGVD is a fixed reference adopted as a standard geodetic datum for heights. The geodetic datum is fixed and does not take into account the changing stands of sea level. Since the geodetic datum represents a best fit over a broad area, the relation between the geodetic datum and local mean sea level is not consistent from one location to another in either time or space. The last general adjustment taken into account for the data presented in this report was the 1947 adjustment. South Slough is a shallow body of water connected to the system via a single channel between the cities of Charleston on the west and Barview on the east. The upper reaches of South Slough constitute a National Marine Sanctuary, administered by the National Oceanographic and Atmospheric Administration, and the first created under the Coastal Zone Management Act. South Slough is characterized by narrow channels winding their way through mud flats and sandbars. The region to be modeled encompasses an area of over 46 square miles.

---

* A table of factors for converting U. S. customary units of measurement to metric (SI) units is presented on page 3.

5

2.   Traffic into and out of Charleston Harbor has been affected
by the shifting of Charleston Channel (that part of the South Slough
channel from the main Coos Bay channel to Charleston Bridge) out of
project alignment. Continual shoaling problems exist within the chan-
nel. Cost of additional maintenance may warrant installation of struc-
tures that would alleviate the problem. A secondary benefit from such
structures would be a potential reduction in wave damage in the
Charleston boat basin. Such plans must be analyzed regarding their
impact on the tidal hydraulics of the entire system and of South Slough
in particular.

3.   A two-dimensional numerical tidal model (WIFM) developed at the
U. S. Army Engineer Waterways Experiment Station (WES) was used to per-
form the analyses. Due to the nature of the complex geometry of the
Coos Bay area, it was necessary to develop a capability of computing
tidal hydrodynamics on a variable grid system. The technique for this
scheme was taken from Wanstrath[1] and introduced into WIFM.

Objectives

4.   The primary objective of this study was to apply WIFM to the
Coos Bay-South Slough complex to predict quantitatively the hydro-
dynamics (exclusive of sediment transport and wave action) of the tidal
flow in the system, and hence draw a comparison between existing condi-
tions and alternate plan conditions. Specifically, the following tasks
were accomplished:

> a. A field survey for obtaining prototype tidal and velocity
>   data
>
> b. A numerical investigation of tidal circulation including
>   verification and testing of five alternate improvement
>   plans
>
> c. A wave refraction study for the area around the entrance
>   channel

6

PART II: COMPUTATIONAL TECHNIQUES

Equations of Motion

5. The hydrodynamic equations used in this work are the classical shallow-water wave equations. Expressed in a Cartesian coordinate system (Figure 2), the equations of motion are given as

MOMENTUM

$$\frac{\partial U}{\partial t} + \frac{\partial}{\partial x}\left(\frac{U^2}{d}\right) + \frac{\partial}{\partial y}\left(\frac{UV}{d}\right) - fV + gd\frac{\partial \eta}{\partial x} = -\frac{gU}{C^2 d^2}\left(U^2 + V^2\right)^{1/2} + F_x \quad (1)$$

$$\frac{\partial V}{\partial t} + \frac{\partial}{\partial x}\left(\frac{UV}{d}\right) + \frac{\partial}{\partial y}\left(\frac{V^2}{d}\right) + fU + gd\frac{\partial \eta}{\partial y} = -\frac{gV}{C^2 d^2}\left(U^2 + V^2\right)^{1/2} + F_y \quad (2)$$

CONTINUITY

$$\frac{\partial \eta}{\partial t} + \frac{\partial U}{\partial x} + \frac{\partial V}{\partial y} = R \quad (3)$$
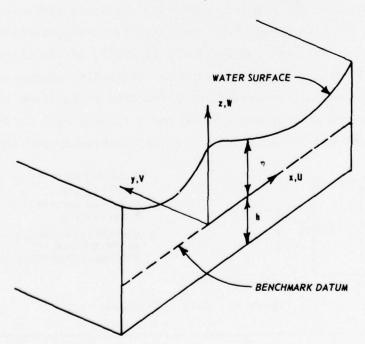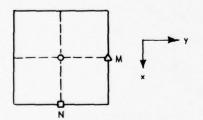
Figure 2.   Coordinate system for problem formulation

7

The fluid has been assumed incompressible and homogeneous and all density variations are neglected. In these equations U and V are the vertically integrated transports per unit of width at time t in the x and y directions, respectively; η is the water-surface elevation with respect to the given datum; $d = \eta - h$ is the total water depth at (x,y,t); f is the Coriolis parameter; C is the Chezy coefficient; F_x and F_y are terms representing external forcing functions such as wind effects; g is the acceleration due to gravity; and R is a term representing the rate at which additional water is introduced into or taken from the system (for example, through rainfall and evaporation).* A complete derivation of these equations can be found in Wang and Connor.[2]

Numerical Approach

6. Since obtaining a solution to the governing nonlinear equations on a highly complex region is intractable for a purely analytical approach, a numerical technique is employed. A finite difference scheme which treats the time dependency implicitly for cost-effective simulation is applied, whereby, the dependent variables of the centered, alternating-direction procedure[3] are the vertically integrated fluid transports and surface elevations as a function of position and time. A space-staggered grid scheme is used and a typical cell is described in Figure 3. Included in the model are actual bathymetry and topography,

□ — FLOW/UNIT WIDTH IN X-DIRECTION (U)

▲ — FLOW/UNIT WIDTH IN Y-DIRECTION (V)

○ — SURFACE ELEVATION (η), WATER DEPTH (d), FRICTIONAL COEFFICIENT (C OR n)

Figure 3. Cell definition

* For convenience, symbols and unusual abbreviations are listed and defined in the Notation (Appendix A).

8

variable bottom roughness, inertial forces due to advective and Coriolis accelerations, rainfall, and spatial and time-dependent wind fields. Flooding of low-lying terrain during a normal tide cycle is simulated. The model is also capable of treating subgrid barrier effects. Exposed, submerged, and overtopping barriers can be represented within the grid system. The formulation of the flooding model (entitled WIFM--WES Implicit Flooding Model) is presented in detail by Butler.[4]

Variable Grid

7. The initial version of WIFM only permitted the use of a regular spaced rectilinear grid system. Due to the nature of the Coos Bay-South Slough complex and the relatively small dimensions of plan modifications to be tested, it was necessary to develop a variable grid procedure to permit economical simulation of the study region. A coordinate transformation given by

$$x = a + b\alpha^c \tag{4}$$

where a , b , and c are arbitrary constants, is applied piecewise for each axis. One may consider this transformation as mapping prototype space, discretized with a smoothly varying grid, into computational space (α-space) employing a regular-spaced grid. The transformation is such that in α-space all derivatives are centered. By applying a smoothly varying grid whose functional as well as first derivatives are continuous, stability problems usually associated with variable grid schemes are eliminated. This type of transformation permits simulation of a complex landscape by locally increasing grid resolution and/or aligning coordinates along physical boundaries.

8. The equations of motion in α-space can be written as

MOMENTUM

$$\frac{\partial U}{\partial t} + \frac{1}{\mu_1} \frac{\partial}{\partial \alpha_1} \left(\frac{U^2}{d}\right) + \frac{1}{\mu_2} \frac{\partial}{\partial \alpha_2} \left(\frac{UV}{d}\right) - fV + \frac{gd}{\mu_1} \frac{\partial \eta}{\partial \alpha_1}$$

$$= -\frac{gU}{C^2 d^2} \left(U^2 + V^2\right)^{1/2} + F_{\alpha_1} \tag{5}$$

9

$$\frac{\partial V}{\partial t} + \frac{1}{\mu_1} \frac{\partial}{\partial \alpha_1} \left(\frac{UV}{d}\right) + \frac{1}{\mu_2} \frac{\partial}{\partial \alpha_2} \left(\frac{V^2}{d}\right) + fU + \frac{gd}{\mu_2} \frac{\partial \eta}{\partial \alpha_2}$$

$$= -\frac{gV}{C^2 d^2}\left(U^2 + V^2\right)^{1/2} + F_{\alpha_2} \qquad (6)$$

CONTINUITY

$$\frac{\partial \eta}{\partial t} + \frac{1}{\mu_1} \frac{\partial U}{\partial \alpha_1} + \frac{1}{\mu_2} \frac{\partial V}{\partial \alpha_2} = R \qquad (7)$$

where

$$\mu_1 = \frac{\partial x}{\partial \alpha_1} = b_1 c_1 \alpha_1^{(c_1 - 1)} \qquad (8)$$

$$\mu_2 = \frac{\partial y}{\partial \alpha_2} = b_2 c_2 \alpha_2^{(c_2 - 1)} \qquad (9)$$

Minor modifications of the finite difference analogs to Equations 1-3 are required to introduce the factors μ_1 and μ_2 appearing in Equations 5-7. The quantities μ_1 and μ_2 define the stretching of the regular-spaced computational grid in α-space (spatial steps of $\Delta\alpha_1$ and $\Delta\alpha_2$) to approximate a study region in real or prototype space (x, y space).

9. A time-share code has been designed to calculate the mapping defined by Equation 4. Each axis is partitioned into any number of regions for which the mapping coefficients are determined. The code allows the user full control over the variable spacing along each axis. Having mapped both spatial directions independently, a batch code plots the variable grid in prototype space on a pen plotter for use as an overlay on bathymetric charts for ease of digitizing water depths. In addition, values for the quantities μ_1 and μ_2 are given on punched cards for direct use by program WIFM.

Boundary Conditions

10. Various types of boundary conditions are permissible in the present code. These include:

    a. Open boundaries. Water levels or flow rates are

prescribed functions of location and time and are given as tabular input to WIFM.

b. Water-land boundaries. Such boundaries lie on cell faces and hence impermeable boundaries are accounted for by specifying $U = 0$ or $V = 0$ at the appropriate cell face. Low-lying terrain may alternately dry and flood within a tidal cycle. Inundation is simulated by making the location of the land-water boundary a function of the current value of the total water depth. By checking water level in adjacent cells relative to ground elevation, a determination is made as to the possibility of inundation. If flooding is possible, the boundary face is treated as open and computations for η , U , and V are made for that cell. Figure 4 depicts a graphic representation of flood cell treatment. The drying of cells is simply the inverse process. The code does allow excess water to drain from "dry cells," noting that inundation or drying occurs when the adjacent water level exceeds or is within some small fraction of a foot (0.2 ft in this application).

c. Subgrid barriers. Subgrid barriers are defined along cell faces and are of three types: exposed, submerged, and overtopping. Exposed barriers are handled by simply spec-ifying no-flow conditions across the appropriate cell face. Submerged barriers are simulated by controlling the flow across cell faces with the use of a time-dependent frictional coefficient (Chezy coefficient). Overtopping barrier is a terminology used to distinguish barriers which can be submerged during one portion of the tidal cycle and totally exposed in another. Actual overtopping is controlled by using a broad-crested weir formula[5] to specify the proper flow rate across the barrier. Once the barrier is submerged (or conversely exposed), pro-cedures as described above are followed. Figure 5 gives a graphic description of these barrier conditions.

CELL
INTERFACE

CLOSED

ϵ

$d = \eta - h$

WATER PASSED
TO DRY CELL

ϵ

$d = \eta - h$

OPEN

$\leftarrow$ v

ϵ

$d = \eta - h$
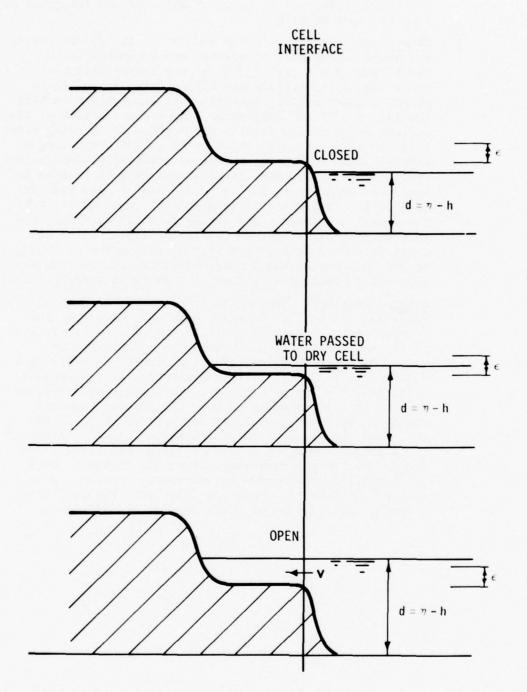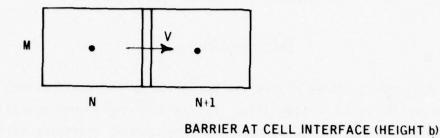
Figure 4.   Flood cell treatment

12

BARRIER AT CELL INTERFACE (HEIGHT b)

EXPOSED

$V = 0$
$\eta_N < b + \epsilon$
$\eta_{N+1} < b + \epsilon$

SUBMERGED

$\eta_N > b + \epsilon$
$\eta_{N+1} > b + \epsilon$
V CONTROLLED BY
SPECIAL CHEZY
COEFFICIENT

OVERTOPPING

$\eta_N > b + \epsilon$
$\eta_{N+1} < b + \epsilon$
$V = C_o d_H \sqrt{d_H}$

WATER IS PASSED TO
LOW SIDE ACCORDING
TO FLOW RATE V
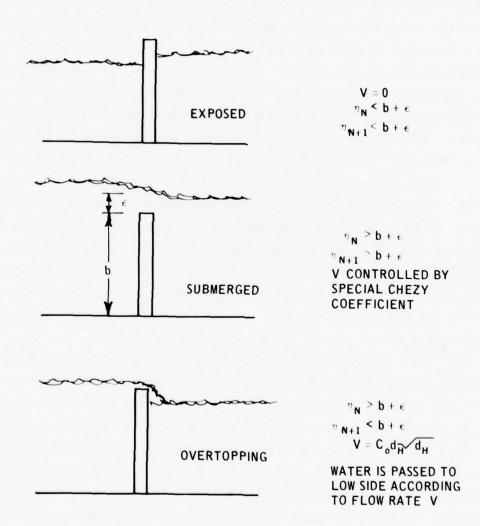
Figure 5. Barrier conditions treated by WIFM

PART III: TIDAL CIRCULATION FOR EXISTING CONDITIONS

Field Survey

11.   A prototype field survey was performed by the staff at WES
during the period 14-22 October 1976. Eleven tide gages were installed,
eight of which were in the model area and were used in verifying WIFM to
existing conditions. An additional gage at Charleston Harbor, monitored
by National Ocean Survey (NOS), was also used in the verification pro-
cess. The gages outside the model limits were installed to aid NOS in
establishing Charleston as a NOS reference station. In turn, NOS pro-
vided technical assistance in establishing the proper benchmarks for all
gages installed. A 25-hour velocity survey was carried out on 21-22
October.   Current and salinity measurements were taken at 10 locations
within 5 ranges. Figure 6 depicts all model tide gage locations and
velocity range and station locations. The velocity survey was conducted
under a calm sea condition. Since the calm survey period is the only
scenario to be modeled and proposed modifications will not affect wind-
driven circulation in South Slough, wind effects have been neglected in
the study. A concurrent effort by NPPEN to gather hydrographic survey
data provided definition of the existing bathymetry. The datum selected
for WIFM was 1947 NGVD since most bathymetric charts provided were re-
lated to this datum.

12.   Tidal gages located at Cape Arago (gage 1) and Empire (gage 0)
were used to provide data for driving the numerical model at open-water
boundaries (Figure 6). Tidal readings at Cape Arago contained a great
deal of high-frequency components. In order to extract meaningful tidal
data from actual readings, a least-squares harmonic (LSH) fit to eight
days of available data was made. Figure 7 depicts the Cape Arago LSH
fit for the duration of the velocity survey. The same process was also
applied to the OSU gage (gage 2) and the fitted data were used for com-
parison with model results.

14
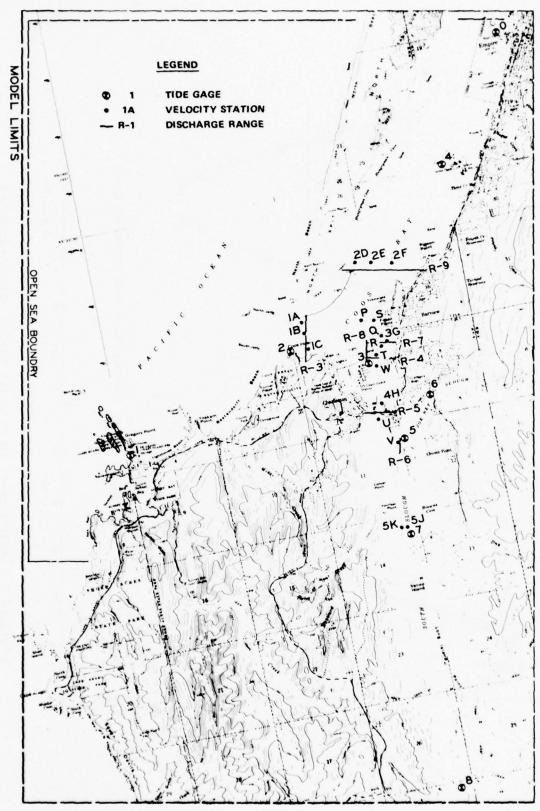
Figure 6. Extent of model area, gage, and range locations
for Coos Bay Inlet/South Slough
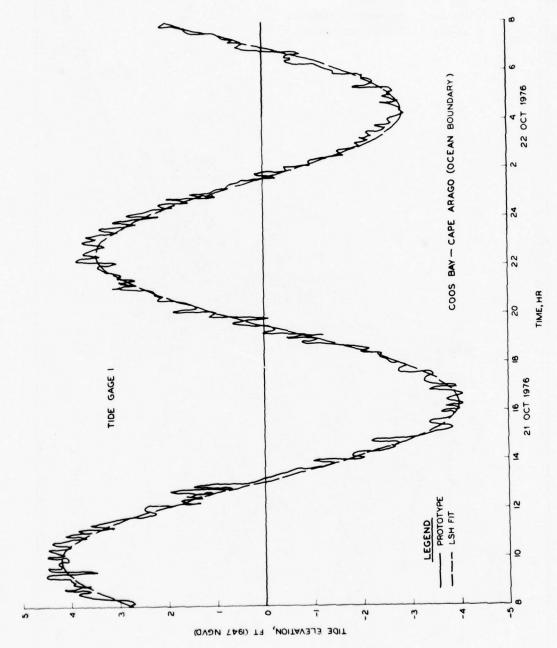
Figure 7. Least-squares harmonic fit to Cape Arago tide data

16

Computational Grid

13. The first step in applying WIFM to the study region was to select a computational grid. A variable mesh for each direction was selected with the prototype grid spacing ranging from 150 ft to 900 ft. The finer mesh was focused around the inlet entrance and Charleston Harbor where proposed structures to be tested would likely be placed. Figure 8 shows the computing grid overlaid on an area map. The grid consists of 13,130 incongruent cells having dimensions of 130 x 101. Recall that a coordinate transformation in the form of a piecewise "exponential squeeze" is applied independently to each axial direction to map the variable grid into an equally spaced computing grid used directly by WIFM.

14. Fourteen bathymetry maps of the model area were reduced to the same scale (1:6000) and pieced together to form three maps: Empire to Charleston Harbor, Charleston Harbor to the south end of South Slough, and the open ocean area. Grid overlays for digitizing water depths were generated and plotted on a Calcomp drum plotter. Depth and keyed bottom characteristics (for defining associated Manning's n) were tabulated for each grid cell.

15. As mentioned previously, the open ocean boundary was forced with the tide history obtained at Cape Arago, and the open water boundary near Empire was forced with the tide history taken at a nearby dock. All other boundaries were taken as movable land-water boundaries. The effects of small channels entering the southernmost end of South Slough were neglected since their effect on comparing alternate plan conditions with existing conditions would be small.

16. Various subgrid anomalies exist throughout the system, such as boat docks, loading docks, narrow shoals, submerged jetties, exposed jetties, and bridges. These features are treated as barriers described by different frictional coefficients to simulate their effect on circulation.

17
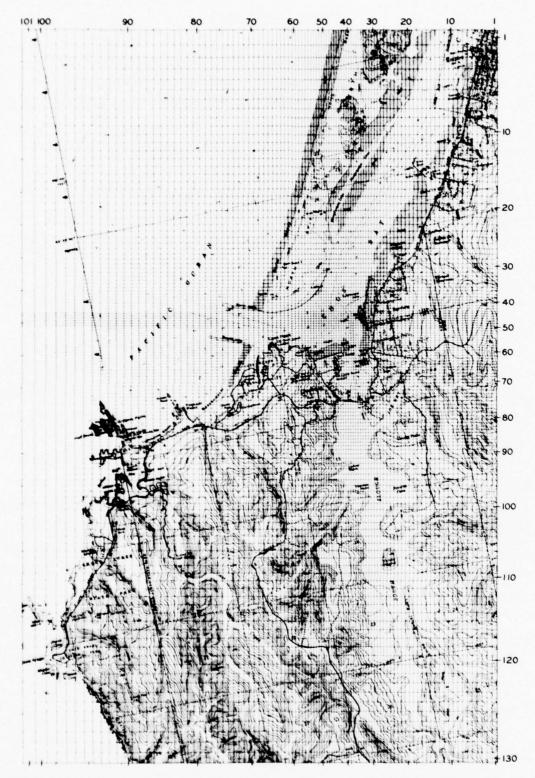
Figure 8.   Computational grid for the Coos Bay model

Model Verification

17. The objective of the verification phase of any model study is to demonstrate the model's ability to produce results that agree with known data for existing conditions. Conditions for the model area from 0800 PST on 21 October to 0800 PST on 22 October were simulated to establish the model's predictive capability as well as base conditions for comparing effects of proposed improvement plans. Comparisons between prototype and model were made for tidal elevations at 9 locations and current velocities at 10 stations. Prototype current measurements were taken at three depths: surface, middepth, and bottom as exemplified in Figure 9. These field data all indicate that neglecting velocity variations in the vertical direction (an assumption used in formulation of the numerical model) is reasonable and justified for the study area. For ease of presentation, comparison between model and prototype velocities will be made by using the prototype middepth velocity.

18. *Surface elevation results are depicted in Plates 1-3 for gages 0-8.* Prototype data for both tide and velocity comparisons are depicted by a solid line and model results by a line annotated with the symbol x. All data were plotted at half-hour intervals. As mentioned previously, gages 0 and 1 were used to drive the numerical model and therefore show excellent agreement. Note that the Cape Arago gage (gage 1) is well removed from the model boundary. Results indicate that its use as a driving gage is a reasonable assumption. All tide gages outside of South Slough show very good agreement between model and prototype. Gages within South Slough (5-8) depict a good comparison although an overshoot in the flood phase is noted. This is probably due to the cruder grid representation used in the slough and the inability to define mud flats and other storage areas accurately due to lack of prototype data. Gage 8 is representative of the hydrograph at Hinch Bridge. Because of the large size of computational cells at the south end of the slough, gage 8 cannot be simulated as accurately as other gages. The variable computation grid was designed to give finer resolution in the area of proposed structural changes. Fine resolution throughout the study area would

19
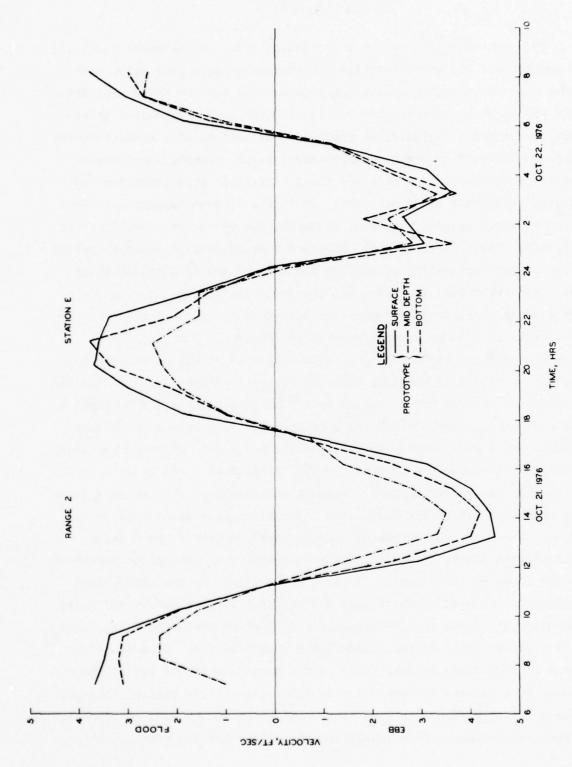
Figure 9. Example of the vertical variation in prototype current measurements

have resulted in a much larger number of grid points forcing WIFM storage requirements to exceed the capacity of the Cyber 176, the fastest and largest computer currently available to the Corps. The grid selected permits an economical and accurate assessment of plan effects relative to base conditions.

19. Velocity comparisons for ranges 1-5 are presented in Plates 4-7. It should be noted that the numerical model began computing from a quiescent state at 0600 PST. It takes about four hours for the model to spin up. This fact would explain the poorer comparison in the first hours of the velocity survey. Some of the prototype data are missing due to operational problems in rough seas. Comparison with prototype velocity data for most ranges and stations is good (recall that the middepth reading at all stations is used for a comparison basis). Range 1 extends from Coos Head to the north jetty across the inlet throat. Range 2 is located between Pigeon Point and North Spit across Coos Bay. The low flood velocity in the second flood phase at sta 2D is an anomaly which may be due to small eddies not simulated by WIFM. Range 3 is located east of the entrance channel to Charleston Harbor. Again, this area is prone to small eddies as seen in the prototype data at the beginning of each ebb phase. Range 4 is located near the entrance to South Slough. Range 5 is located near Copes Dock in South Slough. For Range 5 the numerical model results show a weak flood velocity and a stronger ebb velocity. Sta 5J is located at the entrance to a small lagoon in front of Copes Dock and sta 5K is located in the main slough channel 200 ft west of sta 5J. There is no indication that a freshwater inflow from the south or an anomalous wind condition caused the large ebb velocity. The difference in tidal range between the first and second cycle appears insufficient to cause the prototype ebb velocity in the first phase whose peak magnitude is four times that experienced in the second ebb phase. Although some differences between prototype data and numerical model predictions occurred, the overall quality of the model verification was good. The greater differences occurred in the areas of cruder spatial resolution. As long as changes in hydraulics caused by the introduction of control structures do not extend into

21

these areas, the verification results can be used, with a high degree of reliability, as base conditions for plan effect comparisons. Hence, for the remainder of the report, verification results will be referred to as base conditions.

20. Additional velocity stations were selected for comparing plan with base conditions. Results will be presented in PART IV of this report. Various ranges for comparison of volumetric discharges also were plotted for use in analyzing plan effects.

21. For plotting circulation patterns, the computational region was subdivided into three areas: Coos Bay River Reach (extending from Empire to Charleston Harbor), South Slough (from Charleston Harbor to Hinch Bridge), and an enlargement of the Inlet/Charleston Harbor area. Two types of flow field plots were made: the first displaying transport vectors and the second displaying velocity vectors (similar to surface current patterns). Plots for each simulation hour were produced on microfiche, 35 mm color film, and black and white film. Plates 8-10 display example circulation patterns (transport and velocity) for the inlet subregion at three time instances in the tidal cycle: ebb, flood, and near slack water. These plots indicate the amount and direction of water flowing through a given cell cross section at a given time. A vector with length equal to a minimum cell width represents a flow per unit width of 100 ft^2/sec (transport plots) and a velocity of 3 ft/sec (velocity plots). A complete set of circulation plots is on file at both WES and NPPEN. A few geographic landmarks have been identified in Plate 8 to aid in plot orientation. Heavy straight lines on each circulation plot depict existing or proposed structures (jetties, breakwaters, bridges, boat docks, etc.). Such features shown in Plates 8-10 are all existing structures.

PART IV: ALTERNATE IMPROVEMENT PLANS

22. For the purpose of reducing maintenance costs associated with the navigation channel into Charleston Harbor, NPPEN has proposed testing five alternate improvement plans. Each plan includes dredging a new straight channel to the harbor as well as some combination of breakwaters and/or groins. Figure 10 displays all plan conditions and major velocity stations used in comparing plan with base conditions. The five alternative plans are summarized as follows:

   a. Plan 1 -- An L-shaped breakwater extending from land at a point approximately 1,000 ft northward from the westward end of the existing breakwater toward Fossil Point for 2,600 ft and then north at a right angle toward North Spit for 1,000 ft and three east-west groins (approximately 400 ft long) located between the existing submerged jetty and the entrance to Charleston Harbor on the east side of Charleston Channel.

   b. Plan A -- A 1,000-ft extension of the existing Charleston breakwater toward the north.

   c. Plan B -- The breakwater extension in plan A and a 400-ft east-west groin located on the east side of the entrance channel at the end of the new extension.

   d. Plan C -- Placement of a groin as described in plan B without the breakwater extension.

   e. Plan D -- Conditions as for plan B with the addition of another 400-ft east-west groin at the entrance of Charleston Harbor.

The new channel for plan 1 would be dredged to -15 ft NGVD, and to -14 ft NGVD for all other plans.

23. Plates 11-19 show the comparison of surface elevations with plans installed using verification results as a base condition. No significant changes are noted between plan and base conditions.

24. Plates 20-29 depict the comparison between plan and base conditions for current velocities at base station locations. Again, no significant changes are noted with any plan installed, with the exception of sta 3G. This station is located between or near groins in plans 1, B, C, and D. As expected, the velocity is reduced with the installation of groins east of the new channel.
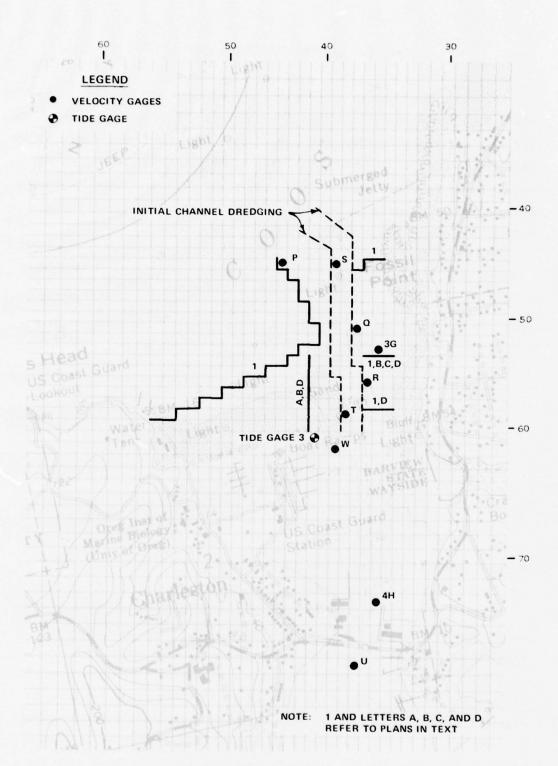
Figure 10. Proposed plans for Coos Bay Inlet with
major velocity stations depicted

25. Additional velocity stations were selected for comparing plan with base conditions. Station locations (P, ... , W) are shown in Figure 6 and results are depicted in Plates 30-37. Sta P is located at the tip of the L-shaped breakwater in plan 1 and the velocity at sta P is reduced by introducing the plan. Since the breakwater extension in plans A, B, and D does not reach the area of sta P, little change is noted with the introduction of these plans. Sta Q and R are located between or near training dikes in all plans except plan A. Results indicate the suppression of flow in these areas. Sta S is located at the confluence of the main channel and the Charleston Harbor (CH) channel. Little change is noted with the introduction of plans AD. However, plan 1 greatly increases the local velocity and discharge into and out of the CH channel since the tip of the L-shaped breakwater nearly reaches this junction. Sta T is located in the CH channel adjacent to the end of the present Charleston breakwater. Introduction of a groin east of the channel will greatly increase the current velocity in the channel as noted in plans 1 and D. Sta U is at the entrance to South Slough and sta V at the entrance to Joe Ney Slough. No significant velocity change is noted with the introduction of any of the proposed plans. Sta W is located in the CH channel at the entrance to the boat basin. Introduction of a groin opposite the end of the present Charleston breakwater slightly increases current velocity into and out of the boat basin.

26. Plates 38-67 display vector flow patterns (transport and velocity) at three time instances in the tidal cycle for each plan. Proposed structures are depicted by additional heavy straight lines in comparison with Plates 8-10. Also given are difference plots (transport and velocity) for each plan. These differences were formed by subtracting vector components of base calculations from plan results. The direction of the resulting vector will be reversed relative to the proper flow direction if the flow magnitude for the base condition is greater than that for plan conditions. All difference plots indicate that the impact on circulation due to plan installment is confined to a localized area near the structures.

27. Several discharge ranges were selected to present graphs of volumetric discharge as a function of time. Plates 68-72 depict the discharge through five ranges (R3-R6, R9) whose locations are given in Figure 6. No change is noted with the installation of any plan for R3 and R9 (inlet throat and Coos Bay-Empire ranges, respectively). Ranges R4, R5, and R6 are located at the entrance to Charleston Harbor, South Slough, and Joe Ney Slough, respectively. Little change in total discharge is noted for these ranges, with plan 1 showing the largest impact at any one instant in time. Results from these and other ranges indicate that the tidal prism in South Slough will not be altered by construction of any of the plans tested.

PART V: WAVE REFRACTION ANALYSIS

Methodology

28. A wave refraction analysis was performed to determine wave
energy levels penetrating the entrance to Coos Bay Inlet. This phase of
the study was conducted using a linear wave refraction program developed
by Dobson.[6] Effects of both reflection and diffraction are neglected,
and thus it is assumed that no energy is transmitted along the wave
crest. These assumptions lead to the wave height being defined by the
relation

$$H = H_o K_s K_r$$

where H_o is the wave height in deep water, K_s is the shoaling co-
efficient, and K_r is the refraction coefficient. Refraction diagrams
were produced from two grids as depicted in Plate 73. The open ocean
grid extends seaward to water depths of 600 ft and the inlet entrance
grid extended from the seaward end of the jetties forming the inlet
entrance to Barview. The inlet grid was developed to compute the dis-
position of wave energy penetrating the inlet.

Deepwater Grid Results

29. Wave orthogonals were calculated and plotted from initial
deepwater directions SW, WSW, W, WNW, NW, and NNW, and for periods of
8, 10, 12, 14, 16, and 18 sec. Figures for the deepwater refraction
patterns were assembled in a separate report to NPPEN. Plates 74-79
display samples from each deepwater direction. Table 1 summarizes the
results for this phase of the analysis. Values given in the table are
representative of an average of orthogonals in the harbor entrance.
The wave-height adjustment factor is the product of K_s and K_r , and
can be applied to any deepwater wave height to obtain the corresponding
shallow-water wave height. Since linear theory breaks down in

27

convergence areas, a maximum refraction coefficient of 1.4 and a minimum of 0.4 should be taken as reasonable limiting values.[7]

Inlet Grid Results

30. For four deepwater directions, SW, WSW, NW, and NNW, the direction of the shallow-water wave at the inlet opening was at such an angle that the computer code could not compute orthogonals extending much beyond Coos Head just inside the inlet entrance. Four examples are depicted in Plates 80-83 for a period of 12 sec. The wave front azimuth at the inlet opening was computed by averaging the shallow-water azimuths for each deepwater direction. The shallow-water azimuths used in the inlet grid runs are tabulated below.

Deepwater Direction	Shallow-Water Azimuth
SW (225°)	272.5^o
WSW (247.5^o)	276.5^o
Average of W and WNW (270° and 292.5^o)	297.5^o
NW (315°)	315.5^o
NNW (337.5^o)	321.5^o

31. Wave energy approaching the interior of the bay is concentrated from directions W to WNW (75 percent) as given by National Marine Consultants.[8] The average shallow-water azimuth resulting from these deepwater directions is 297.5^o. Since shallow-water waves from such an azimuth begin propagating directly up the entrance channel, these conditions were considered the ones in which maximum wave energy would reach the Barview area. Refraction diagrams for wave periods from 8-18 sec are given in Plates 84-90. Note that two figures are presented for the 14-sec period. The second diagram (Plate 88) indicates the sensitivity in choosing the spacing between wave orthogonals at the beginning of the computation. Since each wave ray is computed independently, it is possible to compute crossovers as exhibited. One can consider each ray as

28

representing the movement of a "packet" of energy, and thus it is not inconsistent for such crossovers to occur. The results obtained by the linear wave refraction code are very limited for sites such as Coos Bay due to the complex channel formation extending outward from the inlet jetties and shoal areas adjacent to the main channel as it progresses toward Barview.

PART VI: CONCLUSIONS

32. The Coos Bay-South Slough numerical model was verified to re-
produce satisfactorily the hydrodynamic response of the Coos Bay inlet
system to a specified astronomical tide. The verification procedure
substantiates the model's ability to reliably predict the impact of
proposed modifications to the Charleston Channel area on tidal eleva-
tions, current velocities, and circulation within the study region.

33. Results of the five plans tested show that construction of
any of these improvement plans tested will have a minimal effect on
tidal circulation in South Slough; most velocity and circulation changes
concerned with these plans were confined to the local vicinity of the
proposed modifications. The greatest effect on the hydrodynamics of the
total system would occur with construction of plan 1. Results for plans
A-D indicate that the combination of a Charleston breakwater extension
and one or more groins on the east side of Charleston Channel would best
meet the District's needs. These plans are less expensive to construct
than plan 1 yet still permit control over alignment of the Charleston
Channel.

34. No conclusions regarding reduction of shoaling problems in the
Charleston Channel or of wave damage in the Charleston boat basin can be
made. The tidal circulation model is not designed to address these
problems and wave refraction models are severely limited by inherent
assumptions of no energy transfer across wave orthogonals. Consequently
results from wave refraction analyses are of limited value in quanti-
tatively evaluating the effect of various plans on wave energy in
Charleston boat basin. However, inspection of the circulation patterns
and wave refraction analyses coupled with experienced coastal engineer-
ing judgment may lend some insight into these problems.

REFERENCES
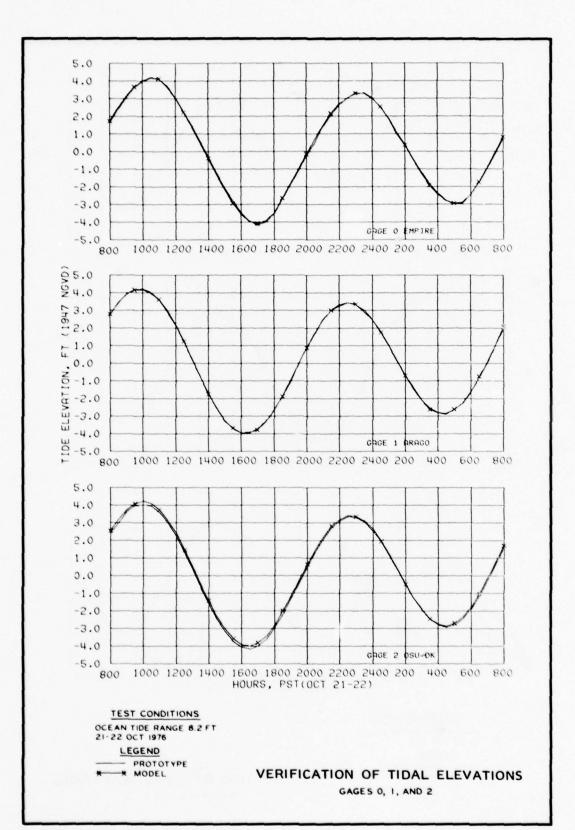
1. Wanstrath, J. J., "Nearshore Numerical Storm Surge and Tidal Simulation," Technical Report H-77-17, Sep 1977, U. S. Army Engineer Waterways Experiment Station, CE, Vicksburg, Miss.

2. Wang, J. D. and Connor, J. J., "Mathematical Modeling of Near Coastal Circulation," Report No. 200, Apr 1975, Ralph M. Parsons Laboratory for Water Resources and Hydrodynamics, Massachusetts Institute of Technology, Cambridge, Mass.

3. Leendertse, J. J., "A Water-Quality Simulation Model for Well-Mixed Estuaries and Coastal Seas; Vol 1, Principles of Computation," RM-6230-rc, Feb 1970, Rand Corporation, Santa Monica, Calif.

4. Butler, H. L., "Numerical Simulation of Tidal Hydrodynamics: Great Egg Harbor and Corson Inlets, New Jersey," Technical Report H-78-11, Jun 1978, U. S. Army Engineer Waterways Experiment Station, CE, Vicksburg, Miss.

5. Reid, R. O. and Bodine, B. R., "Numerical Model for Storm Surges in Galveston Bay," Journal, Waterways and Harbors Division, American Society of Civil Engineers, Vol 94, No. WW1, Paper 5805, Feb 1968, pp 33-57.

6. Dobson, R. S., Some Applications of a Digital Computer to Hydraulic Engineering Problems, M.S. Thesis, Stanford University, Stanford, Calif., 1967.

7. Whalin, R. W., "The Limit of Applicability of Linear Wave Refraction Theory in a Convergence Zone," Research Report H-71-3, Dec 1971, U. S. Army Engineer Waterways Experiment Station, CE, Vicksburg, Miss.

8. National Marine Consultants, Inc., "Wave Statistics for Three Deep Water Stations Along the Oregon-Washington Coast," May 1961, Santa Barbara, Calif.; Prepared for U. S. Army Engineer District, Portland, CE, Portland, Oreg.
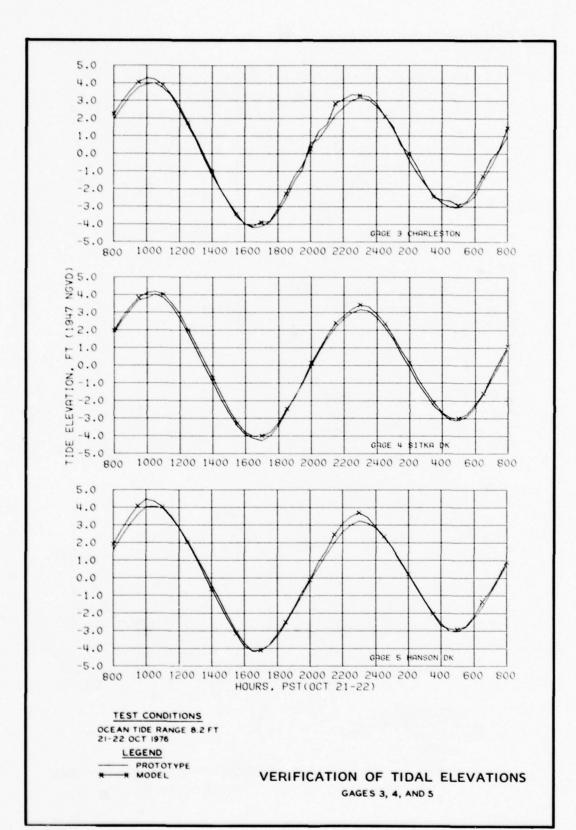
Table 1
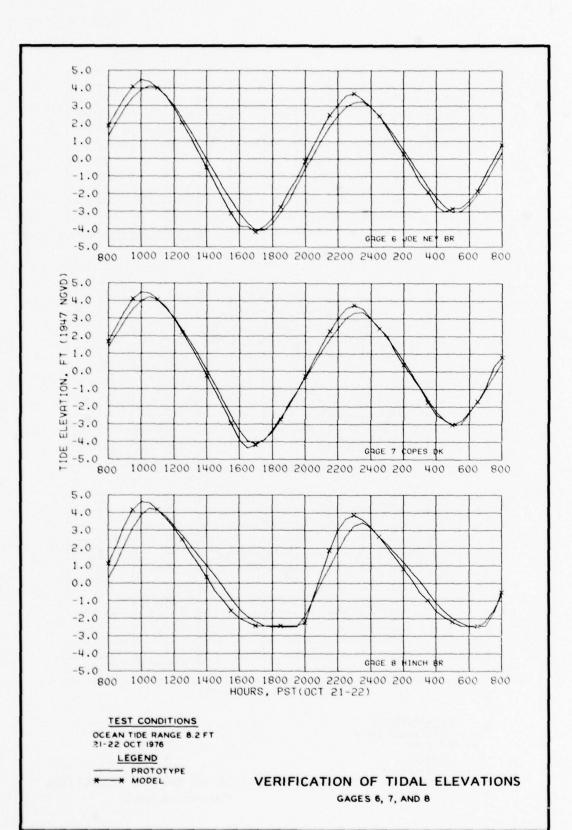
Summary of Refraction and Shoaling Analysis at the

Entrance of Coos Bay Harbor, Oregon
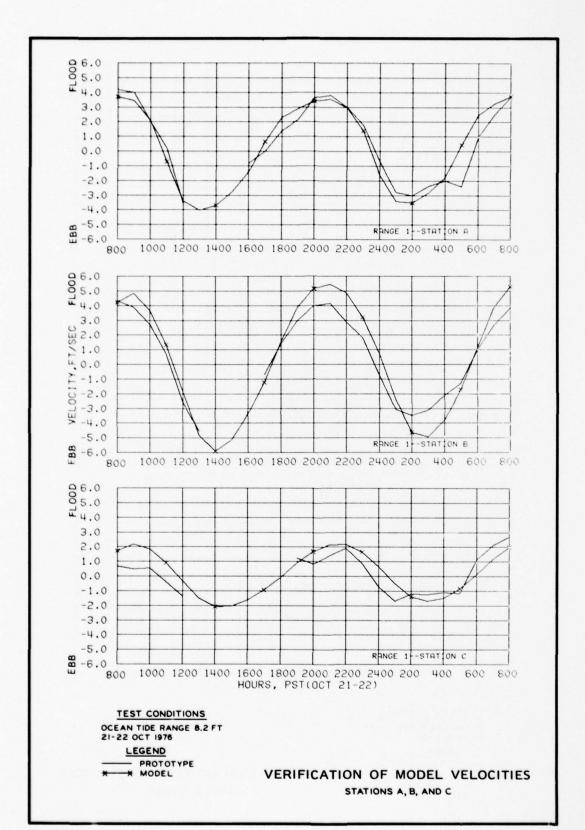
Deepwater Direction	Wave Period sec	Shallow-Water Azimuth deg	Refraction Coefficient	Shoaling Coefficient	Wave-Height Adjustment Factor
SW(225°)	8	268	0.48	0.95	0.46
	10	263	0.30*	1.01	0.30
	12	267	0.26*	1.08	0.28
	14	279	0.58	1.09	0.63
	16	280	0.67	1.11	0.74
	18	278	0.66	1.34	0.88
WSW(247.5°)	8	266	0.38*	0.96	0.37
	10	270	0.58	0.96	0.56
	12	274	0.73	1.08	0.79
	14	278	0.66	1.14	0.75
	16	282	0.61	1.17	0.71
	18	289	0.48	1.17	0.56
WEST(270°)	8	281	0.86	0.97	0.83
	10	288	0.62	0.98	0.61
	12	291	0.68	1.02	0.69
	14	295	0.46	1.10	0.51
	16	297	0.41	1.11	0.46
	18	299	0.80	1.22	0.98
WNW(292.5°)	8	302	0.71	0.93	0.66
	10	303	0.62	0.97	0.60
	12	300	1.01	1.03	1.04
	14	301	0.77	1.08	0.83
	16	305	0.92	1.11	1.02
	18	307	1.10	1.16	1.28
NW(315°)	8	315	0.84	0.95	0.80
	10	313	0.70	1.00	0.70
	12	315	0.76	1.03	0.72
	14	316	0.58	1.05	0.61
	16	317	0.72	1.18	0.85
	18	317	0.52	1.19	0.62
NNW(337.5°)	8	323	0.97	0.94	0.91
	10	327	0.81	1.00	0.81
	12	322	0.71	1.01	0.72
	14	318	0.62	1.10	0.68
	16	320	0.56	1.13	0.63
	18	319	0.61	1.20	0.73
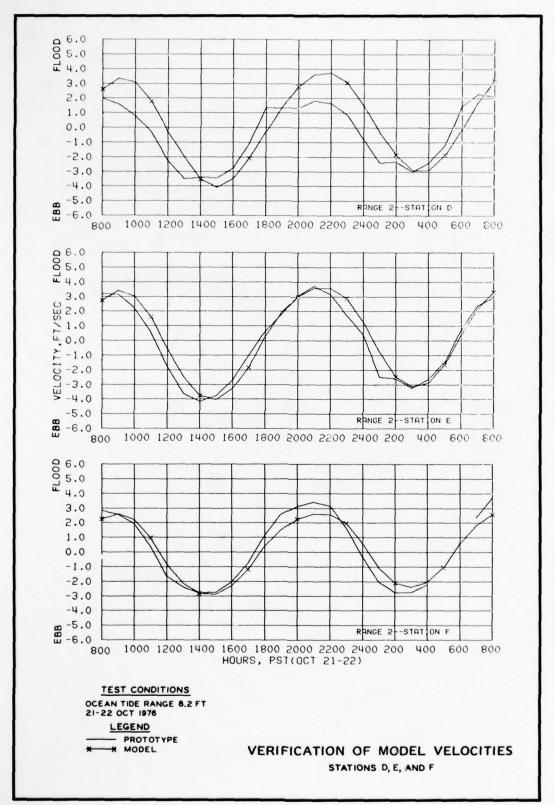
* A minimum refraction coefficient of 0.40 should be used.

VERIFICATION OF TIDAL ELEVATIONS

GAGES 0, 1, AND 2

PLATE 1

VERIFICATION OF TIDAL ELEVATIONS

GAGES 3, 4, AND 5

TEST CONDITIONS

OCEAN TIDE RANGE 8.2 FT
21-22 OCT 1976

LEGEND

———— PROTOTYPE
——— MODEL

PLATE 2

TEST CONDITIONS

OCEAN TIDE RANGE 8.2 FT
21-22 OCT 1976

LEGEND

——— PROTOTYPE
—— MODEL

VERIFICATION OF TIDAL ELEVATIONS

GAGES 6, 7, AND 8

PLATE 3

VERIFICATION OF MODEL VELOCITIES
STATIONS A, B, AND C

PLATE 4

VERIFICATION OF MODEL VELOCITIES
STATIONS D, E, AND F

PLATE 5

FLOOD

VELOCITY, FT/SEC

EBB

6.0
5.0
4.0
3.0
2.0
1.0
0.0
-1.0
-2.0
-3.0
-4.0
-5.0
-6.0

800 1000 1200 1400 1600 1800 2000 2200 2400 200 400 600 800

RANGE 3--STATION G

RANGE 4--STATION H

HOURS, PST(OCT 21-22)

TEST CONDITIONS

OCEAN TIDE RANGE 8.2 FT
21-22 OCT 1976

LEGEND

———— PROTOTYPE
—— MODEL

VERIFICATION OF MODEL VELOCITIES

STATIONS G AND H

PLATE 6

TEST CONDITIONS

OCEAN TIDE RANGE 8.2 FT
21-22 OCT 1976

LEGEND

———— PROTOTYPE
—— MODEL

VERIFICATION OF MODEL VELOCITIES

STATIONS J AND K

PLATE 7

FOSSIL POINT

CHARLESTON

NORTH SPIT

FLOW

VELOCITY
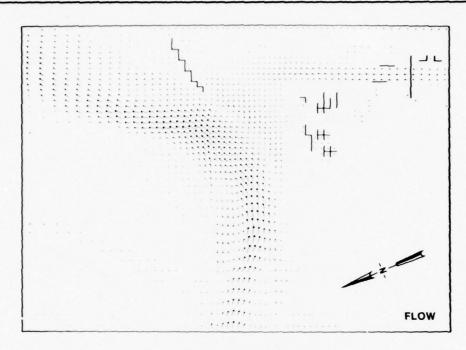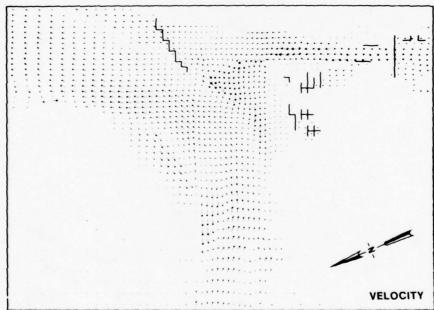
CURRENT PATTERNS
VERIFICATION
HOUR 1400

PLATE 8

FLOW

VELOCITY

CURRENT PATTERNS
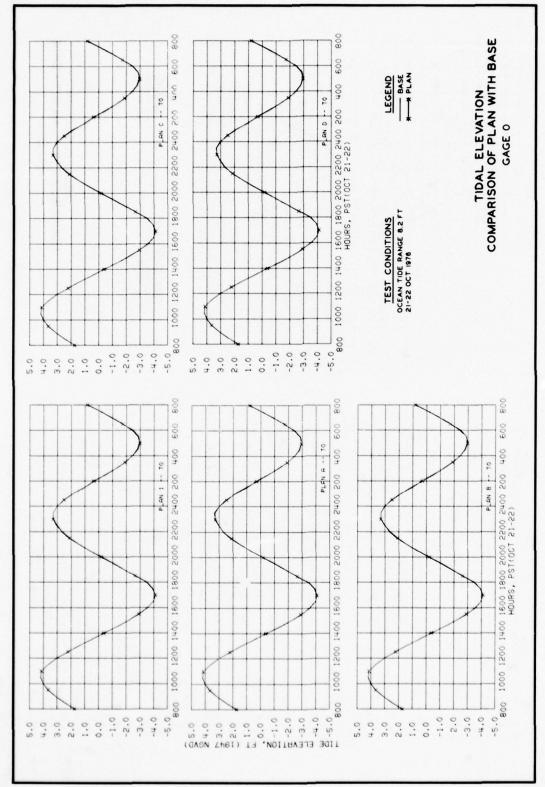
VERIFICATION

HOUR 2100

PLATE 9

FLOW

VELOCITY

CURRENT PATTERNS
VERIFICATION
HOUR 2400

PLATE 10

TIDAL ELEVATION
COMPARISON OF PLAN WITH BASE
GAGE 0

LEGEND
——— BASE
——*—— PLAN

TEST CONDITIONS
OCEAN TIDE RANGE 8.2 FT
21-22 OCT 1976

PLATE 11

TIDAL ELEVATION
COMPARISON OF PLAN WITH BASE
GAGE 1

TEST CONDITIONS
OCEAN TIDE RANGE 8.2 FT
21-22 OCT 1978

LEGEND
—— BASE
—*— PLAN

PLATE 12

TIDAL ELEVATION
COMPARISON OF PLAN WITH BASE
GAGE 2

LEGEND
BASE
PLAN

TEST CONDITIONS
OCEAN TIDE RANGE 8.2 FT
21-22 OCT 1976

PLATE 13

TIDAL ELEVATION
COMPARISON OF PLAN WITH BASE
GAGE 3

TEST CONDITIONS
OCEAN TIDE RANGE 8.2 FT
21-22 OCT 1976

LEGEND
————— BASE
——*—— PLAN

PLATE 14

TIDAL ELEVATION
COMPARISON OF PLAN WITH BASE
GAGE 4

LEGEND
BASE
PLAN

TEST CONDITIONS
OCEAN TIDE RANGE 8.2 FT
21-22 OCT 1976

PLATE 15

TIDAL ELEVATION
COMPARISON OF PLAN WITH BASE
GAGE 5

PLATE 16

LEGEND
BASE
PLAN

TEST CONDITIONS
OCEAN TIDE RANGE 8.2 FT
21-22 OCT 1976

TIDAL ELEVATION
COMPARISON OF PLAN WITH BASE
GAGE 6

PLATE 17

TIDAL ELEVATION
COMPARISON OF PLAN WITH BASE
GAGE 7

PLATE 18

TIDAL ELEVATION
COMPARISON OF PLAN WITH BASE
GAGE 8

TEST CONDITIONS

OCEAN TIDE RANGE 8.2 FT.
21-22 OCT 1974

LEGEND

BASE
PLAN

PLATE 19

VELOCITIES
COMPARISON OF PLAN WITH BASE
STATION IA

PLATE 20

VELOCITIES
COMPARISON OF PLAN WITH BASE
STATION IB

LEGEND
——— BASE
——✕—— PLAN

TEST CONDITIONS
OCEAN TIDE RANGE 8.2 FT
21-22 OCT 1976

PLATE 21

VELOCITIES
COMPARISON OF PLAN WITH BASE
STATION IC

TEST CONDITIONS
OCEAN TIDE RANGE 8.2 FT
21-22 OCT 1976

LEGEND
BASE
PLAN

PLATE 22

VELOCITIES
COMPARISON OF PLAN WITH BASE
STATION 2D

PLATE 23

VELOCITIES
COMPARISON OF PLAN WITH BASE
STATION 2E

LEGEND
BASE
PLAN

TEST CONDITIONS
OCEAN TIDE RANGE 8.2 FT
21-22 OCT 1976

PLATE 24

VELOCITIES
COMPARISON OF PLAN WITH BASE
STATION 2F

LEGEND
—— BASE
—*— PLAN

TEST CONDITIONS
OCEAN TIDE RANGE 8.2 FT
21-22 OCT 1976

PLATE 25

VELOCITIES
COMPARISON OF PLAN WITH BASE
STATION 3G

PLATE 26

VELOCITIES
COMPARISON OF PLAN WITH BASE
STATION 4H

PLATE 27

VELOCITIES
COMPARISON OF PLAN WITH BASE
STATION 5J

TEST CONDITIONS
OCEAN TIDE RANGE 8.2 FT
21-22 OCT 1976

LEGEND
——— BASE
—— PLAN

PLATE 28

VELOCITIES
COMPARISON OF PLAN WITH BASE
STATION 5K

LEGEND
——— BASE
—•— PLAN

TEST CONDITIONS
OCEAN TIDE RANGE 8.2 FT
21-22 OCT 1978

PLATE 29

VELOCITIES
COMPARISON OF PLAN WITH BASE
STATION P

PLATE 30

VELOCITIES
COMPARISON OF PLAN WITH BASE
STATION Q

LEGEND
——— BASE
—*— PLAN

TEST CONDITIONS
OCEAN TIDE RANGE 8.2 FT
21-22 OCT 1976

PLATE 31

VELOCITIES
COMPARISON OF PLAN WITH BASE
STATION R

LEGEND

BASE
PLAN

TEST CONDITIONS
OCEAN TIDE RANGE 8.2 FT
21-22 OCT 1976

PLATE 32

VELOCITIES
COMPARISON OF PLAN WITH BASE
STATION 5

PLATE 33

VELOCITIES
COMPARISON OF PLAN WITH BASE
STATION T

LEGEND
——— BASE
——*— PLAN

TEST CONDITIONS
OCEAN TIDE RANGE 8.2 FT
21-22 OCT 1975

PLATE 34

LEGEND
BASE
PLAN

TEST CONDITIONS
OCEAN TIDE RANGE 8.2 FT
21-22 OCT 1976

VELOCITIES
COMPARISON OF PLAN WITH BASE
STATION U

PLATE 35

VELOCITIES
COMPARISON OF PLAN WITH BASE
STATION V

LEGEND
——— BASE
——*—— PLAN

TEST CONDITIONS
OCEAN TIDE RANGE 8.2 FT
21-22 OCT 1976

PLATE 36

VELOCITIES
COMPARISON OF PLAN WITH BASE
STATION W

PLATE 37

FLOW

VELOCITY

CURRENT PATTERNS
PLAN 1
HOUR 1400

PLATE 38

FLOW

VELOCITY

CURRENT PATTERNS
PLAN 1
HOUR 2100

PLATE 39

FLOW

VELOCITY

CURRENT PATTERNS
PLAN 1
HOUR 2400

PLATE 40

FLOW

VELOCITY

CURRENT DIFFERENCE PATTERNS

PLAN 1 MINUS BASE

HOUR 1400

PLATE 41

FLOW

VELOCITY

CURRENT DIFFERENCE PATTERNS
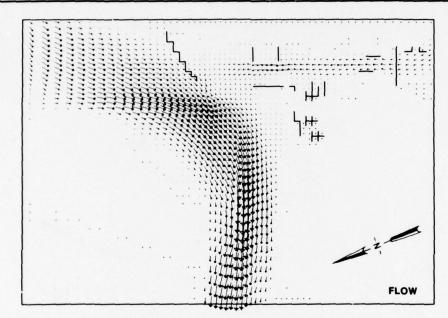
PLAN 1 MINUS BASE

HOUR 2100

PLATE 42

FLOW

VELOCITY

CURRENT DIFFERENCE PATTERNS
PLAN 1 MINUS BASE
HOUR 2400

PLATE 43

FLOW

VELOCITY

CURRENT PATTERNS
PLAN A
HOUR 1400

PLATE 44

CURRENT PATTERNS

PLAN A

HOUR 2100

PLATE 45

FLOW

VELOCITY

CURRENT PATTERNS
PLAN A
HOUR 2400
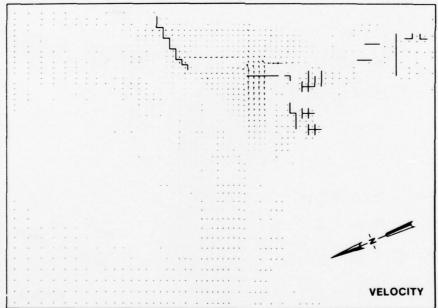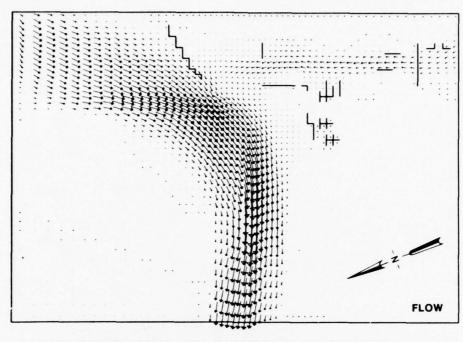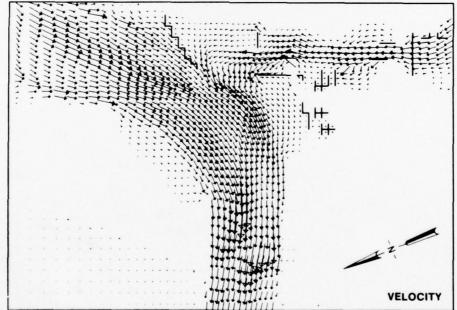
PLATE 46

FLOW

VELOCITY

CURRENT DIFFERENCE PATTERNS
PLAN A MINUS BASE
HOUR 1400

PLATE 47

FLOW

VELOCITY

CURRENT DIFFERENCE PATTERNS

PLAN A MINUS BASE

HOUR 2100

PLATE 48

FLOW

VELOCITY
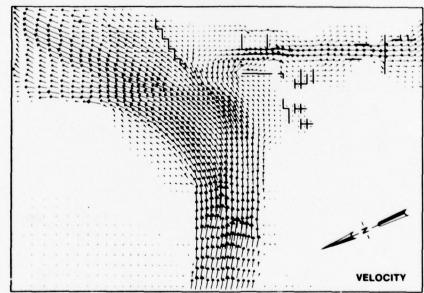
CURRENT DIFFERENCE PATTERNS
PLAN A MINUS BASE
HOUR 2400

PLATE 49

FLOW

VELOCITY
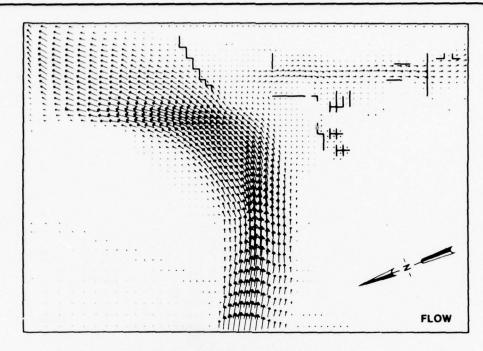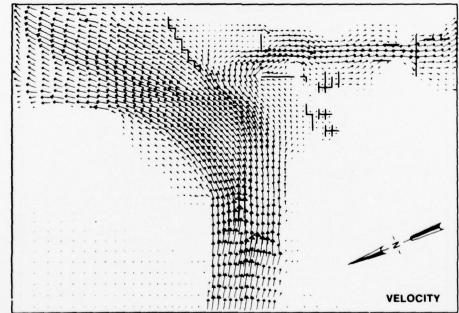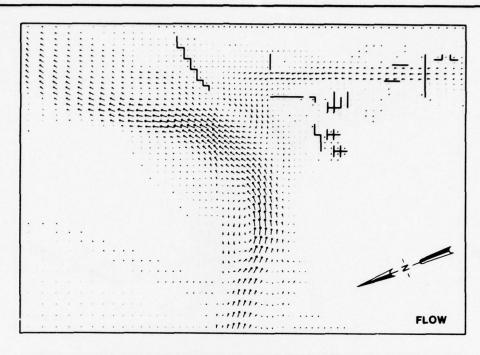
CURRENT PATTERNS

PLAN B

HOUR 1400

PLATE 50

FLOW

VELOCITY
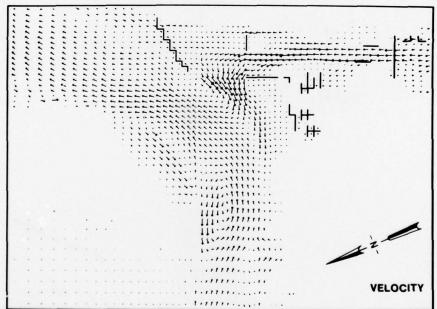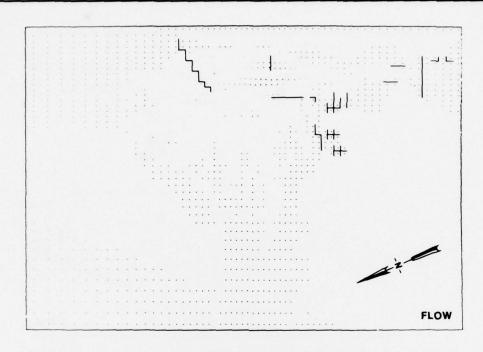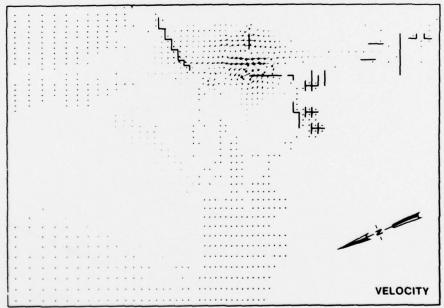
CURRENT PATTERNS
PLAN B
HOUR 2100

PLATE 51

FLOW

VELOCITY

CURRENT PATTERNS
PLAN B
HOUR 2400
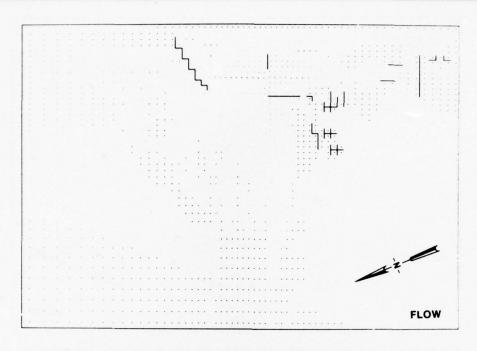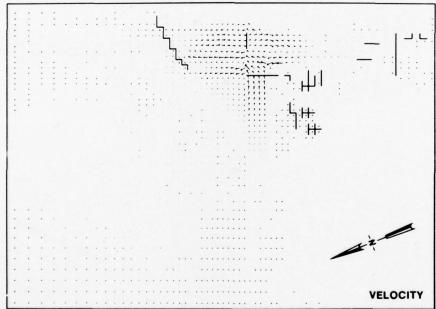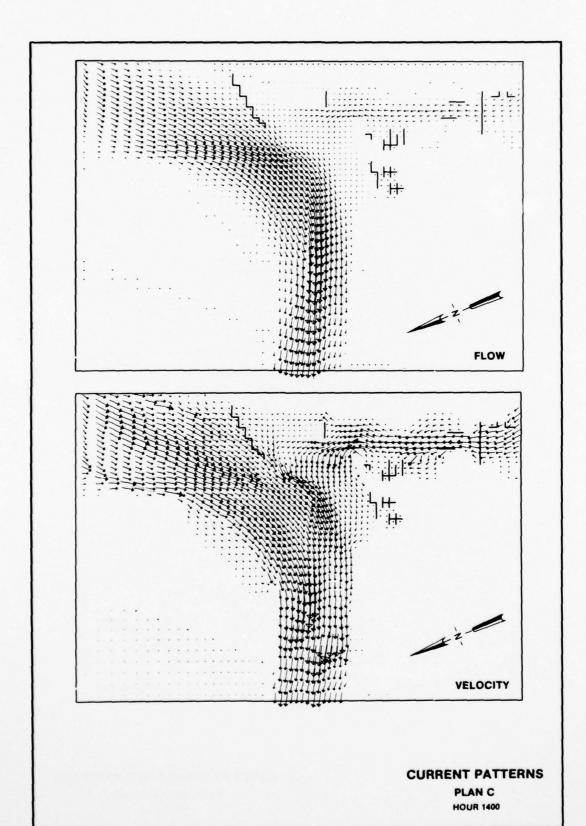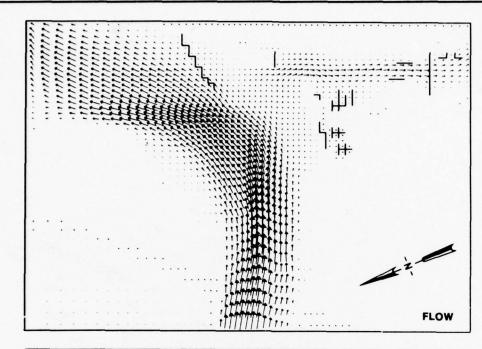
PLATE 52

FLOW

VELOCITY

CURRENT DIFFERENCE PATTERNS
PLAN B MINUS BASE
HOUR 1400

PLATE 53

FLOW

VELOCITY

CURRENT DIFFERENCE PATTERNS
PLAN B MINUS BASE
HOUR 2100

PLATE 54

FLOW

VELOCITY

CURRENT DIFFERENCE PATTERNS
PLAN B MINUS BASE
HOUR 2400

PLATE 55

FLOW

VELOCITY

CURRENT PATTERNS
PLAN C
HOUR 1400

PLATE 56

FLOW

VELOCITY
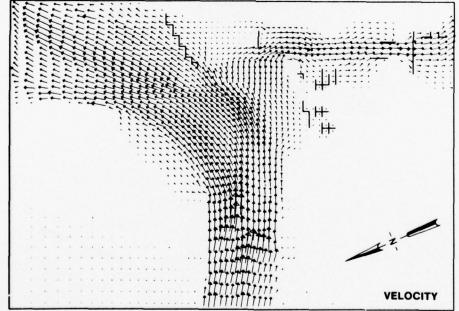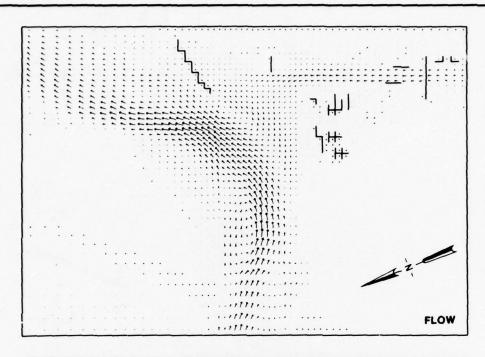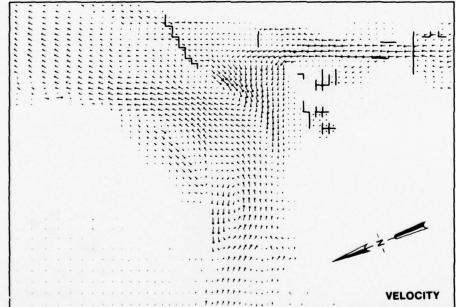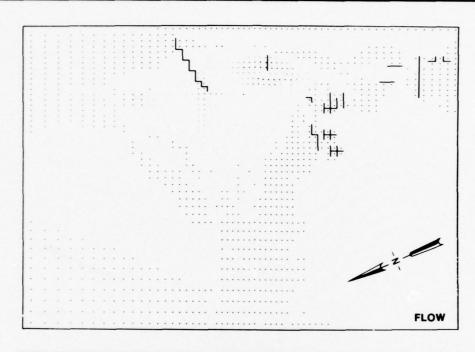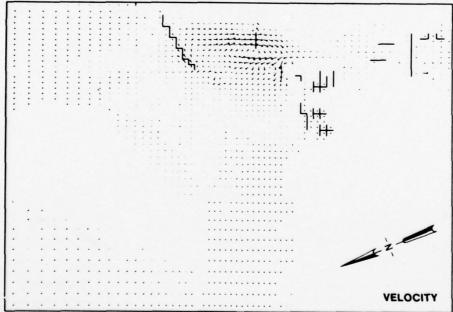
CURRENT PATTERNS
PLAN C
HOUR 2100

PLATE 57

FLOW

VELOCITY

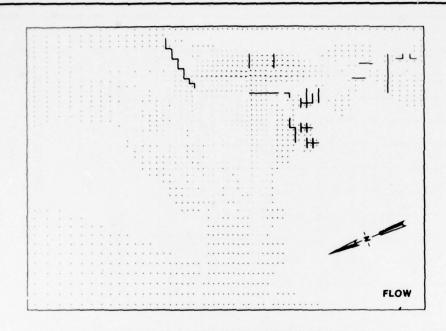**CURRENT PATTERNS**
PLAN C
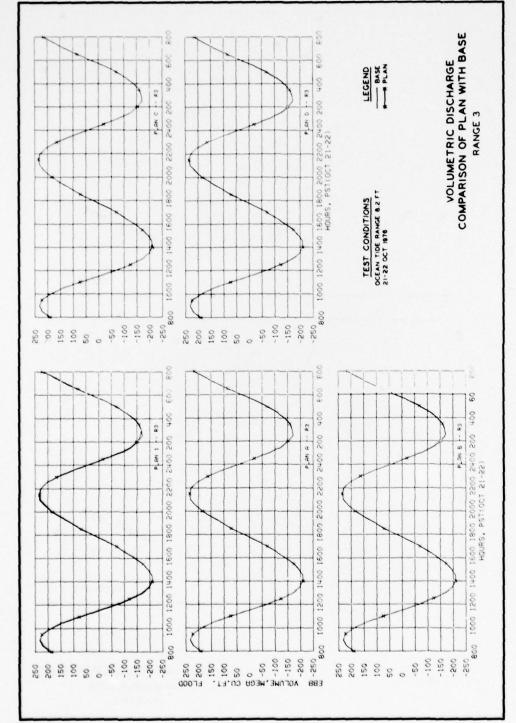**HOUR 2400**
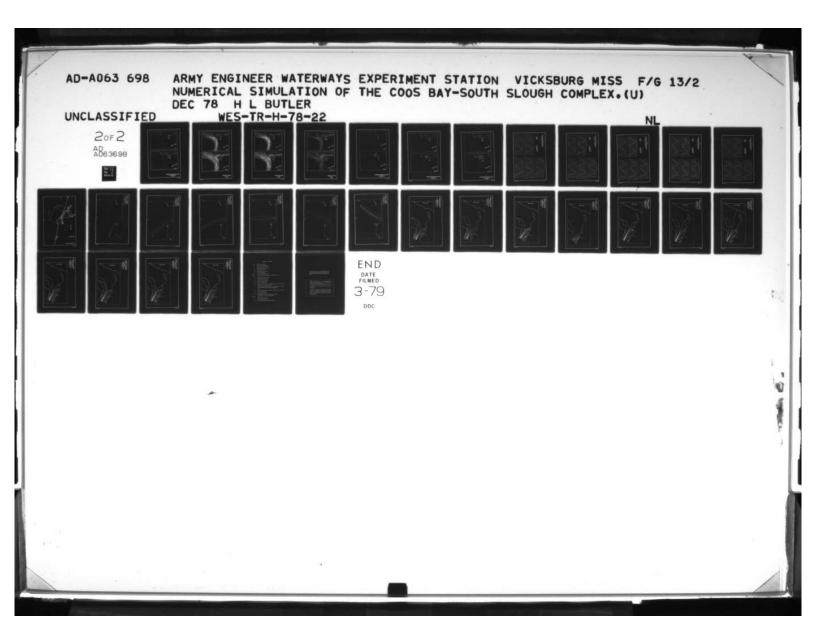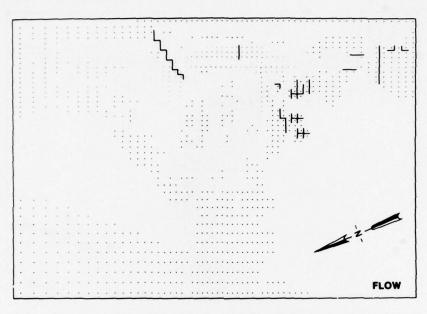
PLATE 58

FLOW

VELOCITY

CURRENT DIFFERENCE PATTERNS
PLAN C MINUS BASE
HOUR 1400

PLATE 59

FLOW

VELOCITY

CURRENT DIFFERENCE PATTERNS
PLAN C MINUS BASE
HOUR 2100

PLATE 60

END
DATE
FILMED

3-79

DDC

FLOW

VELOCITY

CURRENT DIFFERENCE PATTERNS

PLAN C MINUS BASE

HOUR 2400

PLATE 61

FLOW

VELOCITY

CURRENT PATTERNS
PLAN D
HOUR 1400

PLATE 62

FLOW

VELOCITY

CURRENT PATTERNS
PLAN D
HOUR 2100

PLATE 63

FLOW

VELOCITY

CURRENT PATTERNS
PLAN D
HOUR 2400

PLATE 64

FLOW

VELOCITY

CURRENT DIFFERENCE PATTERNS
PLAN D MINUS BASE
HOUR 1400

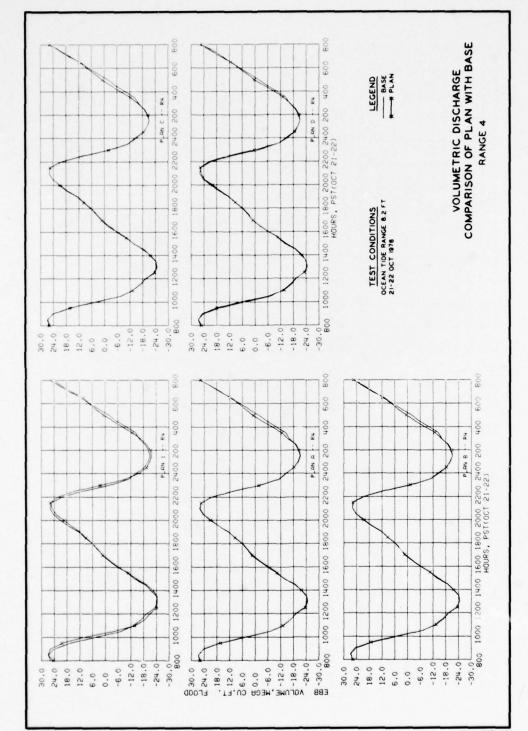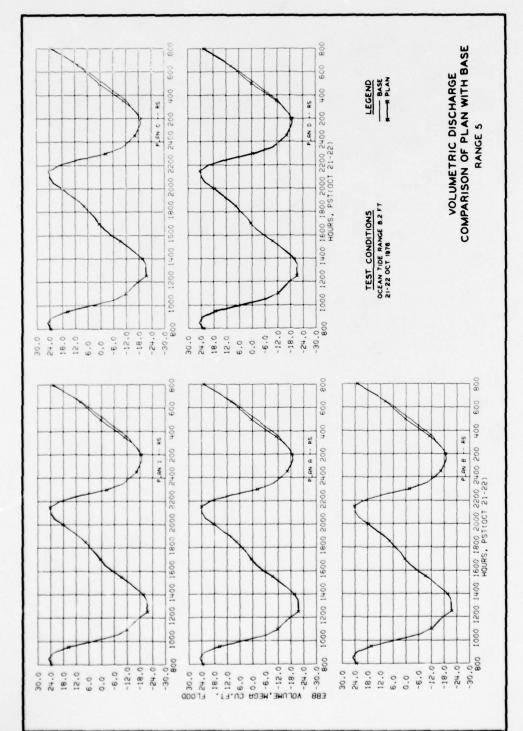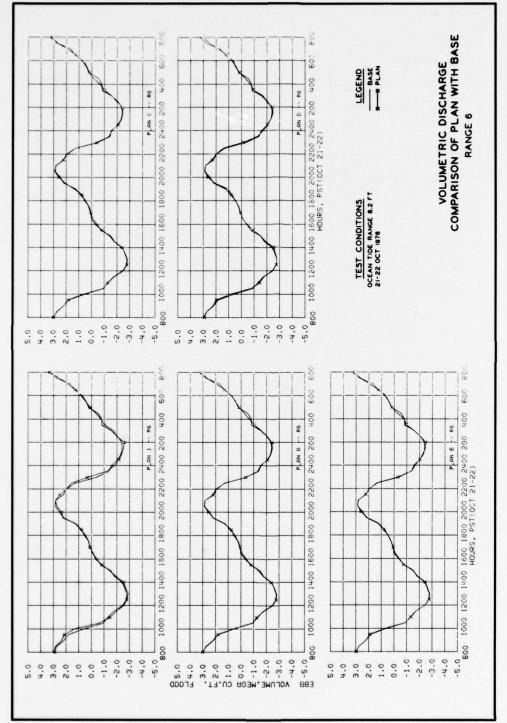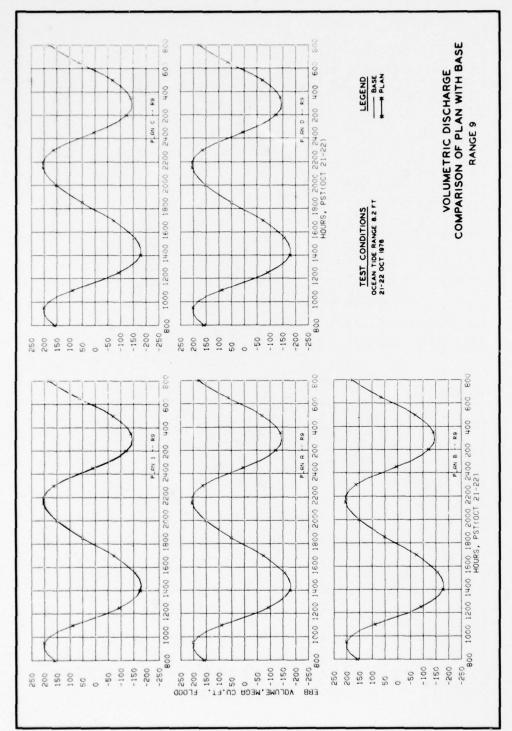PLATE 65

FLOW

VELOCITY

CURRENT DIFFERENCE PATTERNS
PLAN D MINUS BASE
HOUR 2100

PLATE 66

FLOW

VELOCITY

CURRENT DIFFERENCE PATTERNS
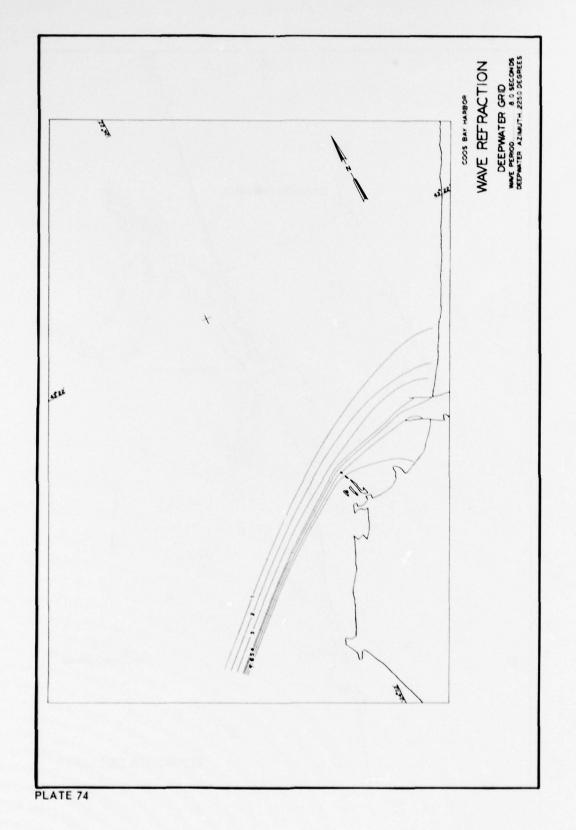
PLAN D MINUS BASE

HOUR 2400

PLATE 67

VOLUMETRIC DISCHARGE
COMPARISON OF PLAN WITH BASE
RANGE 3

PLATE 68

VOLUMETRIC DISCHARGE
COMPARISON OF PLAN WITH BASE
RANGE 4

PLATE 69

VOLUMETRIC DISCHARGE
COMPARISON OF PLAN WITH BASE
RANGE 5

TEST CONDITIONS
OCEAN TIDE RANGE 8.2 FT
21-22 OCT 1976

LEGEND
——— BASE
—*— PLAN

PLATE 70

LEGEND
BASE
PLAN

TEST CONDITIONS
OCEAN TIDE RANGE 8.2 FT
21-22 OCT 1978

VOLUMETRIC DISCHARGE
COMPARISON OF PLAN WITH BASE
RANGE 6

PLATE 71

VOLUMETRIC DISCHARGE
COMPARISON OF PLAN WITH BASE
RANGE 9

TEST CONDITIONS
OCEAN TIDE RANGE 8.2 FT
21-22 OCT 1976

LEGEND
——— BASE
—*— PLAN

PLATE 72

DEEPWATER GRID LIMITS

PACIFIC OCEAN

124° 20'

COOS BAY

INLET GRID LIMITS

43° 20'

OREGON

N

SCALE

1 0 1 2 3 MI

REFRACTION GRID LIMITS

PLATE 73

COOS BAY HARBOR

WAVE REFRACTION

DEEPWATER GRID

WAVE PERIOD............ 8.0 SECONDS
DEEPWATER AZIMUTH 225.0 DEGREES

PLATE 74

COOS BAY HARBOR

WAVE REFRACTION
DEEPWATER GRID
WAVE PERIOD..........10.0 SECONDS
DEEPWATER AZIMUTH 247.5 DEGREES

PLATE 75

COOS BAY HARBOR

WAVE REFRACTION

DEEPWATER GRID
WAVE PERIOD.   120 SECONDS
DEEPWATER AZIMUTH. 2700 DEGREES

PLATE 76

COOS BAY HARBOR

WAVE REFRACTION

DEEPWATER GRID

WAVE PERIOD........14.0 SECONDS
DEEPWATER AZIMUTH:292.5 DEGREES

PLATE 77

COOS BAY HARBOR

WAVE REFRACTION

DEEPWATER GRID
WAVE PERIOD   16.0 SECONDS
DEEPWATER AZIMUTH 3150 DEGREES

PLATE 78

COOS BAY HARBOR

WAVE REFRACTION

DEEPWATER GRID
WAVE PERIOD............18.0 SECONDS
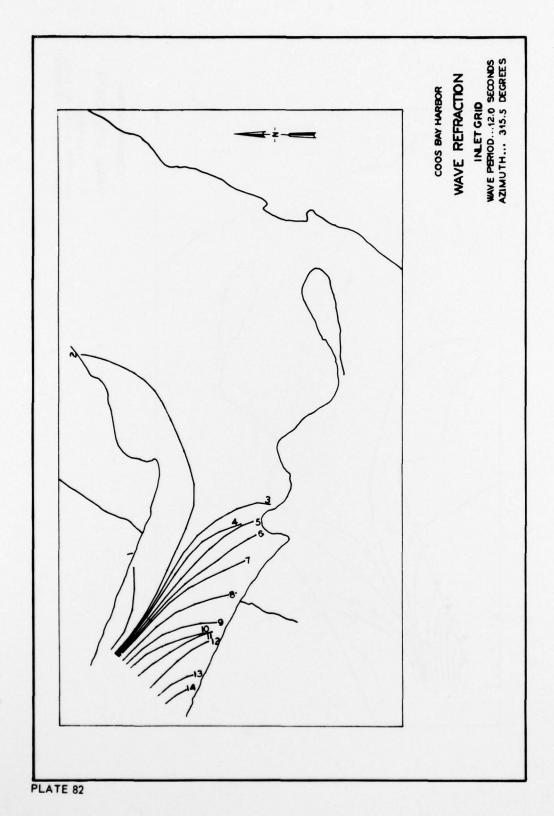DEEPWATER AZIMUTH..3375 DEGREES

PLATE 79

COOS BAY HARBOR
WAVE REFRACTION
INLET GRID
WAVE PERIOD...12.0 SECONDS
AZIMUTH....272.5 DEGREES

PLATE 80

COOS BAY HARBOR

WAVE REFRACTION
INLET GRID
WAVE PERIOD...12.0 SECONDS
AZIMUTH...276.5 DEGREES

PLATE 81

COOS BAY HARBOR

WAVE REFRACTION

INLET GRID
WAVE PERIOD...12.0 SECONDS
AZIMUTH... 315.5 DEGREES

PLATE 82

COOS BAY HARBOR

WAVE REFRACTION

INLET GRID
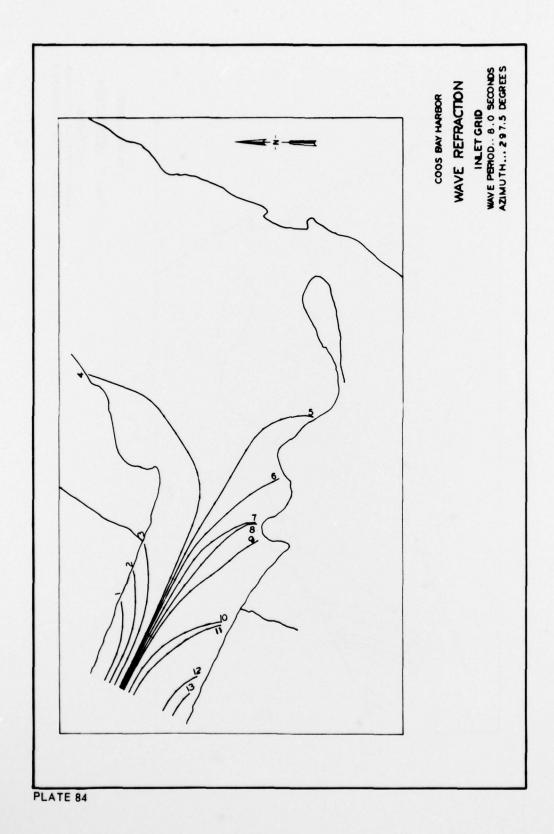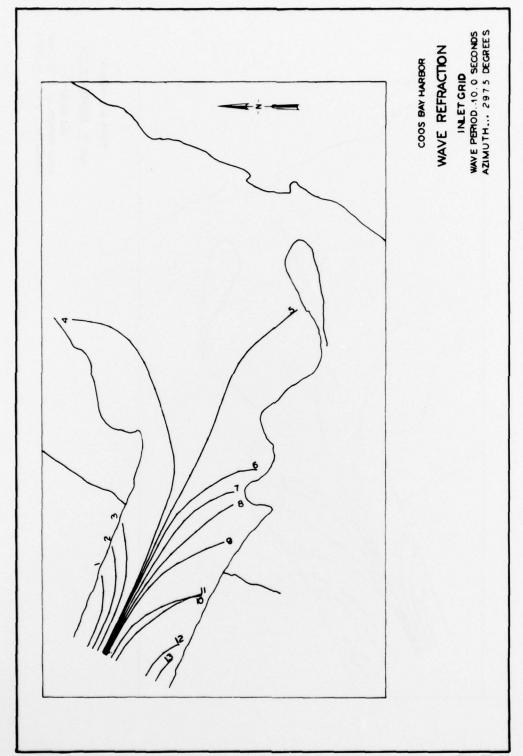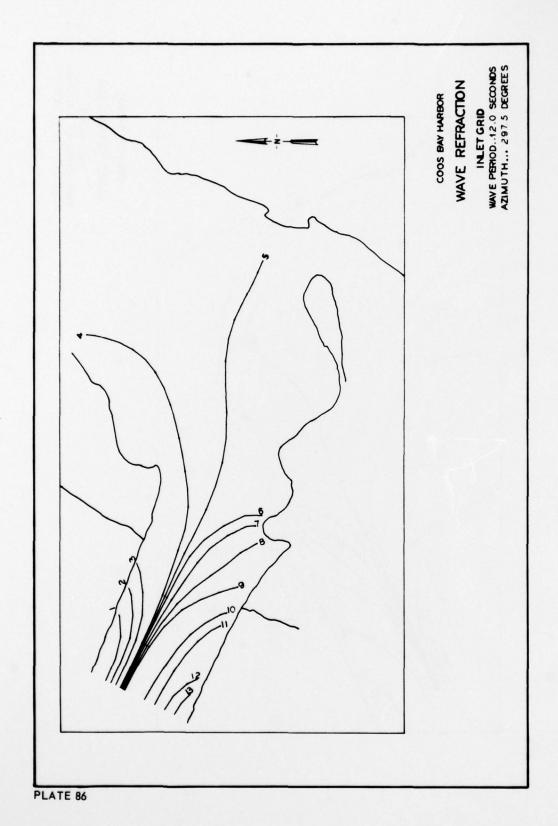WAVE PERIOD...12.0 SECONDS
AZIMUTH... 321.5 DEGREES

PLATE 83

COOS BAY HARBOR

WAVE REFRACTION

INLET GRID

WAVE PERIOD.. 8.0 SECONDS

AZIMUTH.... 2 9 7.5 DEGREES

PLATE 84

COOS BAY HARBOR

WAVE REFRACTION

INLET GRID

WAVE PERIOD..10.0 SECONDS

AZIMUTH.... 297.5 DEGREES

PLATE 85

COOS BAY HARBOR
WAVE REFRACTION
INLET GRID
WAVE PERIOD..12.0 SECONDS
AZIMUTH... 297.5 DEGREES

PLATE 86

PLATE 73

COOS BAY HARBOR

WAVE REFRACTION

INLET GRID

WAVE PERIOD...14.0 SECONDS
AZIMUTH... 297.5 DEGREES

PLATE 87

PLATE 74

COOS BAY HARBOR

WAVE REFRACTION

INLET GRID

WAVE PERIOD..14.0 SECONDS
AZIMUTH...297.5 DEGREES
(SENSITIVITY TEST)

PLATE 88

PLATE 75

COOS BAY HARBOR

WAVE REFRACTION

INLET GRID

WAVE PERIOD...16.0 SECONDS
AZIMUTH....297.5 DEGREES

PLATE 89

PLATE 76

COOS BAY HARBOR

WAVE REFRACTION

INLET GRID

WAVE PERIOD..18.0 SECONDS
AZIMUTH.... 297.5 DEGREES

PLATE 90

PLATE 77
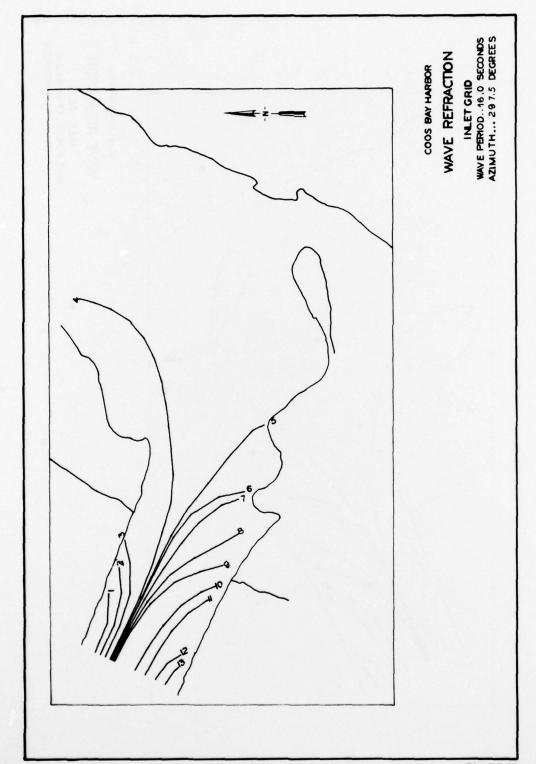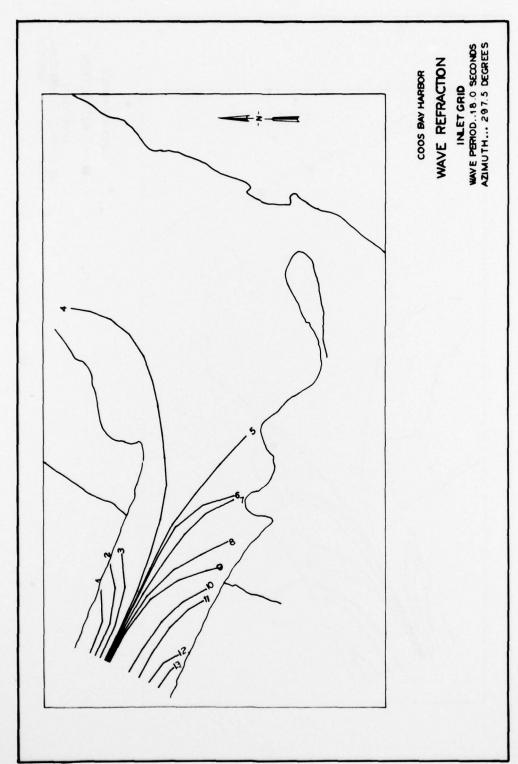
APPENDIX A: NOTATION

a,b,c	Arbitrary constants
b	Barrier height (Figure 5)
C	Chezy frictional coefficient
C_o	Admittance coefficient
d	Total water depth
d_H	Water depth over barrier
f	Coriolis parameter
F_x, F_y	External forcing functions
$F_{\alpha_1}, F_{\alpha_2}$	External forcing functions in computational space
g	Acceleration due to gravity
h	Land-surface elevation
H_o	Wave height in deep water
K_r	Refraction coefficient
K_s	Shoaling coefficient
M,N	Indices denoting spatial increments in the x and y direction
n	Manning's frictional coefficient
R	Rate at which additional water is introduced into or taken from the system (rainfall minus evaporation)
t	Time
U,V	Vertically integrated horizontal transports per unit width
W	Vertical transport
x,y,z	Cartesian coordinates
α	Independent variable in computational space
$\Delta_{\alpha_1}, \Delta_{\alpha_2}$	Spatial steps in computational space
ε	Small depth of water
η	Water-surface elevation
μ_1, μ_2	Grid transformation stretching factors

A1

PLATE 78

In accordance with letter from DAEN-RDC, DAEN-ASI dated
22 July 1977, Subject: Facsimile Catalog Cards for
Laboratory Technical Publications, a facsimile catalog
card in Library of Congress MARC format is reproduced
below.